VIP Poly(A) Duplex Very Important Paper

DOI: 10.1002/anie.201303461

Structure of the Parallel Duplex of Poly(A) RNA: Evaluation of a 50 Year-Old Prediction**

Nozhat Safaee, Anne M. Noronha, Dmitry Rodionov, Guennadi Kozlov, Christopher J. Wilds, George M. Sheldrick, and Kalle Gehring**

The first nucleic acid structure to be elucidated was the B-DNA antiparallel duplex with Watson–Crick base pairs. Although B-DNA is the most common DNA structure, alternative structures, such as A-DNA[1] and Z-DNA,[2] and sequence-specific duplexes,[3–5] triplexes,[6] and quadruplexes[7,8] exist, and in some cases they have been shown to be physiologically relevant.[5] RNA is similarly capable of forming a variety of higher-order structures, including a homopolymer duplex formed by poly(rA), which was first described by Rich, Davies, Crick, and Watson.[9] using diffraction patterns of poly(rA) fibers formed in acidic pH. Based on alternative helical structures of poly(rA) and comparison of the calculated and observed fiber diffraction patterns, they generated the parallel double-helix model of poly(rA), stabilized by N1 protonation. Subsequently, Pattabiraman[10] showed that formation of a parallel, right-handed nucleic acid duplex is thermodynamically favorable. Kikuchi et al.[11] were able to crystallize A-rich fragments of RNA and DNA. Recently, Chakraborty et al.,[12] using NMR spectroscopy and thermal denaturation studies, showed that poly(dA) can form a parallel homo duplex in acidic solution with low salt concentration. Despite time and effort, the detailed atomic structure of the duplex of poly(rA) has remained elusive. Herein, we obtained highly ordered crystals of $(rA)_{11}$ and determined its structure to 1 Å resolution. Thermal denaturation studies were used to study the stability of the poly(rA) duplex in solution and elucidate the conditions for its formation.

[*] N. Safaee, D. Rodionov, Dr. G. Kozlov, Prof. K. Gehring
Department of Biochemistry, McGill University
Montréal, Québec, H3G 0B1 (Canada)
E-mail: nozhat.safaee@mail.mcgill.ca
kalle.gehring@mcgill.ca
Dr. A. M. Noronha, Prof. C. J. Wilds
Department of Chemistry and Biochemistry
Concordia University, Montréal, Québec, H4B 1R6 (Canada)
N. Safaee, Dr. A. M. Noronha, D. Rodionov, Dr. G. Kozlov, Prof. C. J. Wilds, Prof. K. Gehring
Groupe de recherche axé sur la structure des protéines
McGill University, Montréal, Québec, H3G 0B1 (Canada)
Prof. G. M. Sheldrick
Department of Structural Chemistry
University of Göttingen, 37077 Göttingen (Germany)

[**] Primary data collection was done at McGill University. Additional data was collected by Pawel Grochulski and Shaunivan Labiuk at the Canadian Light Source, Saskatoon, SK, Canada and at the Cornell High Energy Synchrotron Source, Ithaca, NY (USA).

Supporting information for this article is available on the WWW under http://dx.doi.org/10.1002/anie.201303461.

Crystallization of $(rA)_{11}$ required the presence of a fragment of poly(A)-binding protein (PABP) containing domains RRM1-2. The binding of $(rA)_{11}$ to the protein most likely reduces the rate of association of the RNA strands to allow the formation of well-ordered crystals. High-quality data were collected from multiple single crystals and initial phases were determined using ab initio direct methods employing the multi-CPU version of the program ShelxD.[13] The structure model was built in Coot[14] and refined using the program ShelxL.[13] The final structure was refined to 1.0 Å resolution (Table 1).

Table 1: Data collection and refinement of the $(rA)_{11}$ duplex structure.[a]

Data collection of $(rA)_{11}$ (PDB ID:4JRD)	
Space group	$P4_12_12$
a, *b*, *c* [Å]	22.8, 22.8, 163.7
Resolution [Å]	22.58–1.0 (1.1–1.0)
R_{merge}	0.094 (0.142)
I/σI	34.4 (4.7)
Completeness [%]	92.6 (73.1)
Redundancy	2.73 (1.20)
Refinement of $(rA)_{11}$	
Resolution [Å]	22.58-1.0 (1.1–1.0)
No. of reflections	22972
R_{work}/R_{free}	0.126/0.158
No. atoms	
poly(A)-RNA	478
water	94
B-factors	
poly(A)-RNA	13.4
water	29.2
RMS deviations[b]	
Bond lengths (Å)	0.007
Bond angles (°)	1.4

[a] Parentheses indicate values for the highest resolution shell.
[b] RMS = root-mean-square.

This structure shows that $(rA)_{11}$ forms a parallel double-stranded helix (Figure 1) with symmetric base pairs formed by two adenine nucleotides (Figure 1 A). The A–A base pairs are "N7-amino-symmetric" where N7 atom of one adenine forms a hydrogen bond with the amino group of the opposite base. This base pairing pattern has been previously observed for the dinucleotide monophosphate of CpA.[15] An additional hydrogen bond forms between the oxygen atom of the phosphate group of one strand and the second hydrogen atom of the amino group from the opposite strand (Figure 1 A). Therefore, the A–A base pairing is mediated by four hydrogen

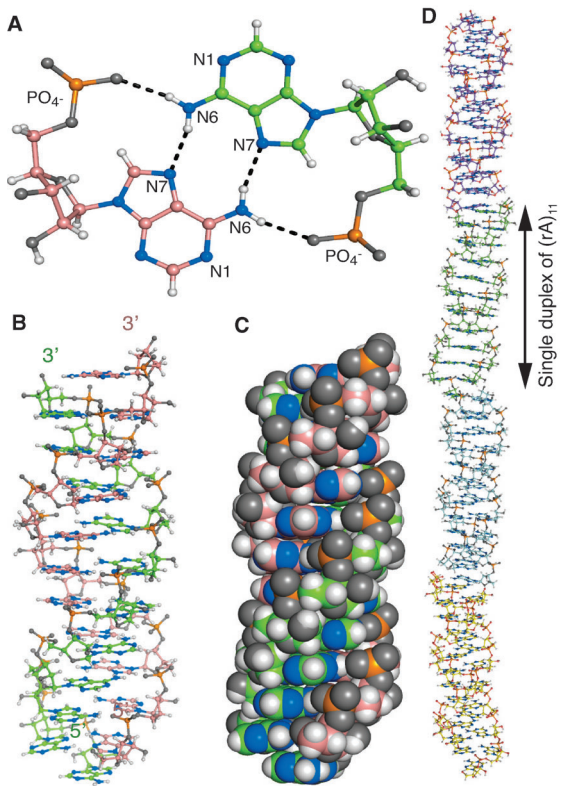

Figure 1. $(rA)_{11}$ forms a parallel, right-handed double-stranded helix. A) The A–A base pair responsible for formation of the poly(rA) duplex. The phosphate groups are driven towards the axis of the helix and form two of the four hydrogen bonds. B) Ball-and-stick representation of the $(rA)_{11}$ duplex. C) The compact structure of $(rA)_{11}$ with a space-filling representation. D) Continuous helix of poly(rA) formed from $(rA)_{11}$ with individual duplexes shown in different colors.

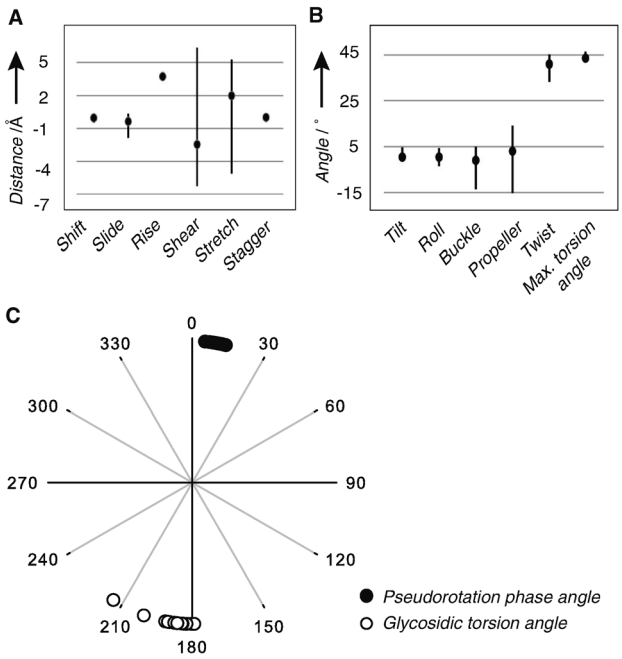

Figure 2. Base-pair and helical properties of the parallel duplex of $(rA)_{11}$. A),B) Distribution and average (filled oval) of base pair and helical parameters in the crystal structure. C) Pseudorotation phase and glycosidic torsion angles.

bonds, engaging the Hoogsteen as well as the Watson–Crick faces of the adenines. These interactions lead to the formation of a parallel double helix where bases are positioned perpendicular to the axis of the helix (Figure 1B). The asymmetric unit of the crystal contains one parallel duplex of $(rA)_{11}$ comprised of ten base pairs and one nucleotide overhanging at each end. The terminal unpaired nucleotides form interduplex base pairs, resulting in a continuous helix (Figure 1D; Supporting Information, Figure S1).

Unlike antiparallel duplexes, with major and minor grooves, the duplex of poly(rA) has grooves of equal size. The glycosidic angle is *trans* (187°), the sugar pucker conformation is 3′-endo with the average pseudorotational phase angle (P) of 10.7° and maximum torsion angle (ν_{max}) of 43.5 (Figure 2). The pitch height, composed of eight base pairs, is 30 Å and the helical rise is 3.7 Å (Figure 2). The formation of the hydrogen bond between phosphate backbone and the adenine base drives the phosphate groups towards the axis of the helix, bringing about the compact structure of the duplex (Figure 1C), in agreement with the fiber diffraction model.[9] To confirm the structure, AnoDe[16] was used to calculate the anomalous density of the backbone phosphorous atoms, using a 1.9 Å dataset collected from a single $(rA)_{11}$ crystal. Such a density is calculated using the measured anomalous differences and phases that are shifted by 90° from the model phases. The resulted anomalous map of the phosphorous atoms agrees with their coordinates in our ab initio model (Supporting Information, Figure S2). Since AnoDe only uses the phases not the structural model, the resulted anomalous map is not model-biased but, independently, confirms the structure.

The stability of the duplex depends on the positioning of the negatively charged phosphate groups proximal to the axis of the duplex to allow formation of hydrogen bonds with the adenine amino groups (Figure 1). Rich et al.[9] suggested that N1 protonation is required to neutralize the charge of the backbone phosphate groups, which is consistent with the fact that they were able to obtain well-ordered fibers at pH 4.

Our structure was however obtained at neutral pH. For 18 nucleotides, we observe strong density for a molecule perfectly positioned to make three hydrogen bonds: one to the purine N1 atom of the same nucleotide, one to the phosphate of the same nucleotide, and one to the phosphate of the preceding nucleotide (Figure 3A,B). The low-temperature factors of these molecules (as low as 13.5 $Å^2$) imply that they are tightly bound as an integral part of the structure, and their close association with the phosphate groups suggests that they could be ammonium ions, which were present in high concentration under the conditions leading to crystallization. As the numbers of electrons in H_2O and NH_4^+ are identical, we cannot distinguish between the two based on electron density.

The absence of ring protonation is supported by careful measurement of the angles and distances in the adenine rings. High-resolution crystallographic studies of adenine nucleosides have shown that the internal angle at N1 is larger when protonated with ranges of 121.9° to 124.1° for protonated and

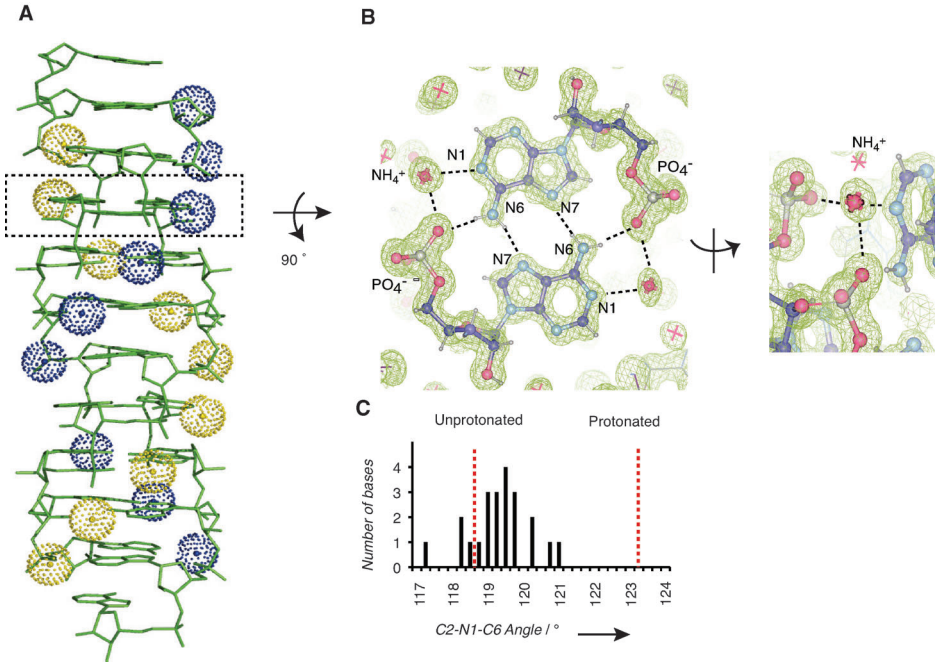

Figure 3. Neutral adenines form homo base-pairs in the presence of ammonium ions. A) Stick representation of the duplex with bound ammonium ions on the two strands shown in yellow and blue dot representations, prepared using PyMol. B) A section of the $2F_o-F_c$ map of the $(rA)_{11}$ structure contoured at 1.3 σ illustrating A–A hydrogen bonds, prepared using Coot.[14] The rotated view of the same section of the map shows that ammonium ion make hydrogen bonds with two phosphate groups from the adjacent nucleotides on the same strand. C) Histogram of the 22 C2-N1-C6 angles in our structure. For comparison, the average values for protonated and neutral adenine are shown.

117.7° to 120.8° for neutral adenine.[17] To measure the C2-N1-C6 angles in our structure, we performed one round of refinement in ShelxL, under relaxed restraints, and used the resulting coordinates to measure the angle. The C2-N1-C6 angles in the duplex range from 117.1° to 120.8°, with a mean value of 119.2° (Figure 3C). This suggests that the adenines are not protonated and that the N1 atoms are available as hydrogen bond acceptors for the bound NH_4^+ (Figure 3B).

To understand the requirement for the poly(rA) duplex formation, we investigated the effects of NH_4^+ and pH on the thermal melting transition (T_m) of poly(rA) duplexes (Figure 4). We found that in the absence of NH_4^+, the duplex of poly(rA) is not stable enough to be detected above pH 5.0 (Supporting Information, Figure S3A). However, the addition of NH_4^+ increased the thermal stability of duplex and the hyperchromatic transition of duplex to single strand was observed even at physiological pH (Figure 4; Supporting Information, Figure S3B). We observed that increasing the concentration of NH_4^+ increased the thermal stability of the poly(A) duplex (Figure 4A). At low concentrations of NH_4^+, the T_m of poly(rA) duplex varies with pH (Supporting Information, Figure S3), suggesting that protonation still plays a role in stabilizing the duplex. However, at a NH_4^+ concentration of 4.4 M, the duplex is stable in a pH-independent manner and could be detected at neutral pH (Figure 4B). It is noteworthy that Na^+ does not stabilize the poly(rA) duplex (Supporting Information, Figure S3D), confirming that hydrogen bond formation between the cations and adenines is essential for stabilizing the A–A base pairs.

Using RNA oligonucleotides of different lengths, we could show that the T_m of poly(rA) duplex increases with its length both at acidic pH in the absence of NH_4^+ and at neutral pH in the presence of NH_4^+ ions (Figure 4C–F). These results show that the A–A base pair formation along the poly(rA) strands is cooperative at both acidic and neutral pH.

The ability of pH and NH_4^+ ions to compensate and cooperatively stabilize the poly(A) parallel duplex suggests that there is fast exchange between the NH_4^+ stabilized duplex reported herein and the H^+ stabilized duplex observed by Rich and colleagues.[9] The structures are likely to be close to isosteric with only minor changes associated with the protonation of the N1 atom and replacement of the bound NH_4^+ ions with water molecules. Thus our crystal structure with 1 Å resolution represents both a confirmation of the original report of a parallel duplex form of RNA and a novel structural motif for supramolecular chemistry.

Parallel poly(rA) duplexes may have played a key role in an early RNA world. Duplex formation could have been a mechanism to regulate ribozyme function upon change of cellular environment. As the great majority of eukaryotic messenger RNAs (mRNA) are tagged with 100 to 250 adenines at their 3′ end, the polymorphism of poly(rA) is also relevant for present day cellular processes involving mRNA translation, storage, and decay. Under conditions of cell stress, cellular mRNAs are transported into RNA granules, increasing the local concentration of poly(rA). It is possible that nature evolved proteins such as PABP in part to regulate the occurrence of poly(rA) duplexes in cells.

Experimental Section

Assembly, purification, and characterization of RNA oligomers, $(rA)_n$, were previously described.[18] Poly(rA) (Sigma–Aldrich) is polyadenylic acid, potassium salt, with an average length of 500 nucleotides. PABP and eIF4G proteins were produced and purified as previously described.[19]

UV thermal denaturation studies: 0.5 OD of poly(rA) was lyophilized and resuspended in buffer, heated to 90 °C for 10 min, cooled slowly to room temperature, and stored at 4 °C overnight before measurements. Denaturation curves were acquired at 260 nm with 0.5 °C min^{-1}, using a Varian CARY Model 3E spectrophotometer. The data were analyzed according to the convention of Puglisi and Tinoco.[20]

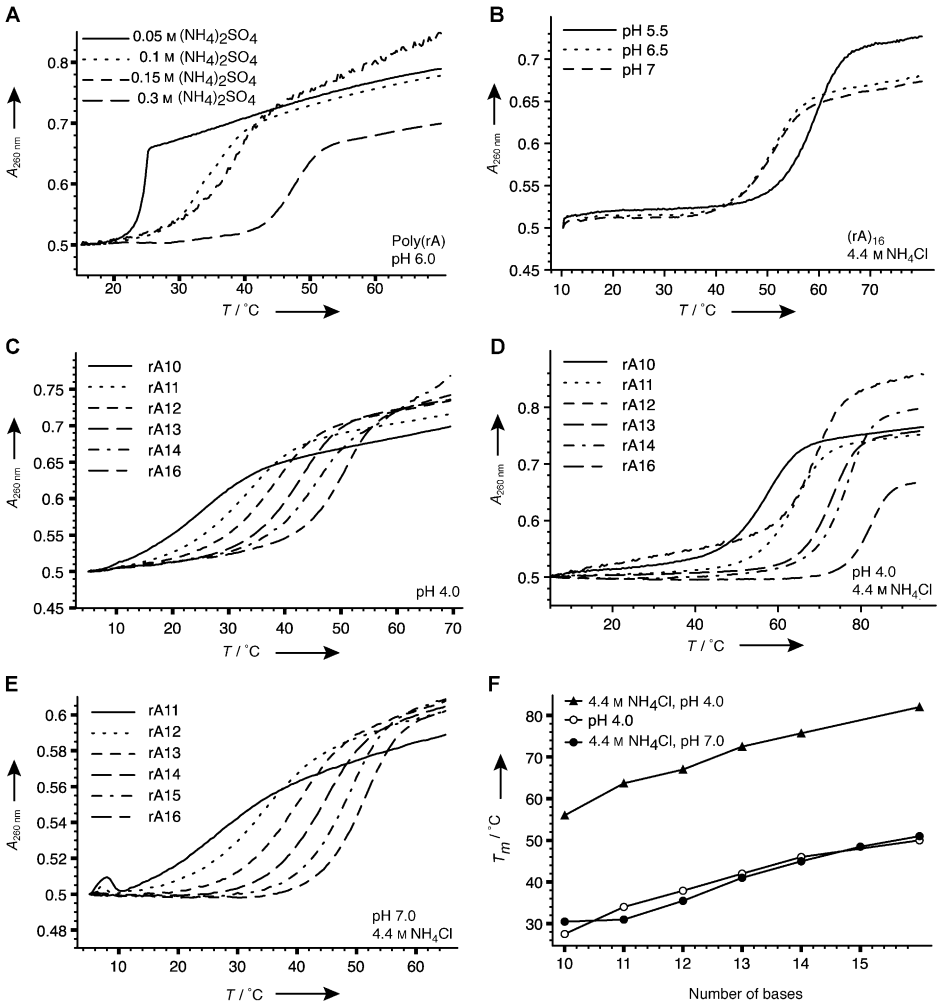

Figure 4. Ammonium ions stabilize the duplex of poly(rA) at physiological pH. A) UV thermal denaturation of long poly(rA) duplexes at 260 nm in 50 mM sodium cacodylate, pH 6.0 supplemented with $(NH_4)_2SO_4$, showing the increase of T_m with higher concentration of $(NH_4)_2SO_4$. B) UV thermal denaturation of $(rA)_{16}$ at 260 nm in the presence of 4.4 M NH_4Cl at the indicated pH. C) UV thermal denaturation of adenylate oligonucleotides with indicated lengths at pH 4.0, D) at pH 4.0, in the presence of 4.4 M NH_4Cl, and E) at pH 7.0 in the presence of 4.4 M NH_4Cl. F) The melting temperatures of oligonucleotides are plotted against the length of oligomers. The absorbances of the samples at 260 nm were normalized to be 0.5 at 10 °C.

Crystals of the $(rA)_{11}$ were obtained using both hanging and sitting drop techniques, by equilibrating a 1 μL drop of the mixture of $(rA)_{11}$:RRM1–2:eIF4G(178–203) in a 1.5:1:3 ratio, in buffer (10 mM HEPES, 50 mM NaCl, 0.5 mM TCEP, pH 7.0), mixed with 1 μL of 2 M $(NH_4)_2SO_4$, 0.2 M NH_4NO_3 at 22 °C. Data were collected from crystals in the cryoprotectant solution (2 M $(NH_4)_2SO_4$, 0.2 M NH_4NO_3 20% (v/v) glycerol) at −180 °C, on a MarMosaic CCD 300 detector at beamline 08ID-1 at the CLS, SK, Canada and A1 beamline at CHESS, Ithaca, USA.

The data sets were processed and scaled anomalously in HKL2000[21] and merged to give improved statistics. The structure was solved using the multi-CPU version of ShelxD.[13] The initial model was completed and adjusted with the program Coot[14] and was improved by several cycles of refinement, using the program ShelxL[13] and model refitting. Anisotropic refinement was carried out in ShelxL by adding the following two lines to the instruction file: 1) ANIS and 2) ISOR HOH 0. The refinement statistics are given in Table 1. The crystals contain one duplex of $(rA)_{11}$ in the asymmetric unit ($Z = 16$) corresponding to V_m of 1.5 $Å^3 Da^{-1}$ and a solvent content of 17.7%.The structure was analyzed using the program 3DNA.[22]

Received: April 23, 2013
Published online: June 27, 2013

Keywords: helical structures · nucleobases · parallel double helix · RNA · structure elucidation

[1] B. Basham, G. P. Schroth, P. S. Ho, *Proc. Natl. Acad. Sci. USA* **1995**, *92*, 6464–6468.
[2] A. H. Wang, G. J. Quigley, F. J. Kolpak, J. L. Crawford, J. H. van Boom, G. van der Marel, A. Rich, *Nature* **1979**, *282*, 680–686.
[3] T. Kobuna, T. Sunami, J. Kondo, A. Takénaka, *Nucleic Acids Res. Suppl.* **2002**, 179–180.
[4] E. M. Evertsz, K. Rippe, T. M. Jovin, *Nucleic Acids Res.* **1994**, *22*, 3293–3303.
[5] K. Rippe, V. Fritsch, E. Westhof, T. M. Jovin, *EMBO J.* **1992**, *11*, 3777–3786.
[6] M. D. Frank-Kamenetskii, S. M. Mirkin, *Annu. Rev. Biochem.* **1995**, *64*, 65–95.
[7] K. Gehring, J. L. Leroy, M. Guéron, *Nature* **1993**, *363*, 561–565.
[8] F. W. Smith, J. Feigon, *Nature* **1992**, *356*, 164–168.
[9] A. Rich, D. R. Davies, F. H. C. Crick, J. D. Watson, *J. Mol. Biol.* **1961**, *3*, 71–86.
[10] N. Pattabiraman, *Biopolymers* **1986**, *25*, 1603–1606.
[11] K. Kikuchi, Y. Sato, E. C. M. Juan, A. Takénaka, *Nucleic Acids Symp. Ser.* **2006**, *50*, 217–218.
[12] S. Chakraborty, S. Sharma, P. K. Maiti, Y. Krishnan, *Nucleic Acids Res.* **2009**, *37*, 2810–2817.
[13] G. M. Sheldrick, *Acta Crystllogr. Sect. A* **2008**, *A64*, 112–122.
[14] P. Emsley, B. Lohkamp, W. G. Scott, K. Cowtan, *Acta Crystallogr. Sect. D* **2010**, *66*, 486–501.
[15] E. Westhof, M. Sundaralingam, *Proc. Natl. Acad. Sci. USA* **1980**, *77*, 1852–1856.
[16] A. Thorn, G. M. Sheldrick, *J. Appl. Crystallogr.* **2011**, *44*, 1285–1287.
[17] R. Taylor, O. Kennard, *J. Mol. Struct.* **1982**, *78*, 1–28.
[18] F. P. McManus, Q. Fang, J. D. M. Booth, A. M. Noronha, A. E. Pegg, C. J. Wilds, *Org. Biomol. Chem.* **2010**, *8*, 4414–4426.
[19] N. Safaee, G. Kozlov, A. M. Noronha, J. Xie, C. J. Wilds, K. Gehring, *Mol. Cell* **2012**, *48*, 375–386.
[20] J. D. Puglisi, I. Tinoco, *Methods Enzymol.* **1989**, *180*, 304–325.
[21] Z. Otwinowski, W. Minor, *Methods Enzymol.* **1997**, *276*, 307–326.
[22] X. Lu, Z. Shakked, W. Olson, *J. Mol. Biol.* **2000**, *300*, 819–840.

